

Experimental and modelling study of the oxidation of methane doped with ammonia

Y. Song¹, O. Herbinet^{1,*}, M. Pelucchi², A. Stagni², T. Faravelli², F. Battin-Leclerc¹

¹ Laboratoire Réactions et Génie des Procédés, CNRS, Université de Lorraine, BP 20451, 1 rue Grandville, 54000 Nancy, France

² Department of Chemistry, Materials and Chemical Engineering “G. Natta”, Politecnico di Milano, P.zza Leonardo da Vinci 32, 20133 Milano, Italy

Abstract

The oxidation of methane doped with ammonia was experimentally and theoretically studied in order to better understand the interactions between these two molecules in combustion processes fed with biogas. Experiments were carried out in a jet-stirred reactor. Several diagnostics were used to quantify reaction products: gas chromatograph for carbon containing species, a NO_x analyzer for NO and NO₂, and continuous-wave cavity ring-down spectroscopy for ammonia. Experimental data were satisfactorily compared with data computed using a model developed by Politecnico di Milano.

Introduction

Biogas is a mixture of different gases produced by the breakdown of organic matter in the absence of oxygen. It primarily consists of methane and carbon dioxide, but it also contains smaller amount of nitrogen, oxygen, water, hydrogen sulfide and ammonia. The composition of biogas depends on the biomass source [1,2].

Ammonia is also an important combustion intermediate during the formation of nitric oxide from nitrogen containing organic fuels. For most solid fuels, ammonia is formed directly during devolatilization [3], and it was also reported as a product of gasification reaction [4].

Most of studies about the oxidation of methane doped with ammonia were performed in premixed flames (e.g., [5,6]). Most of these studies focused on the detection of intermediates formed in flames. Spectroscopic diagnostics like laser-induced fluorescence and intracavity laser absorption spectroscopy were used for the detection of NH₂ [7,8]. Molecular beam mass spectrometry was also used for the analysis of a wider range of products [9]. Henshaw et al. (2005) measured laminar burning velocities of methane flames doped with ammonia [10].

With the increasing interest in biogas fuels as substitutions for fossil fuels, several studies of the oxidation of methane doped with ammonia using carbon dioxide as bath gas have been performed. Konnov et al. studied atmospheric methane flames doped with ammonia and measured nitric oxide (NO) mole fractions in the post-flame zone [5]. A NO/NO₂ chemiluminescence analyzer was used for measuring the NO_x concentration. It was found that the NO_x mole fractions differed qualitatively between CH₄/O₂/N₂ flames and CH₄/O₂/CO₂ flames: NO mole fraction peaked around $\Phi=1$ in the CH₄/O₂/N₂ flames, whereas it peaked under fuel-rich conditions in the CH₄/O₂/CO₂ flames. After that, Mendiara and Glarborg investigated experimentally the oxidation of NH₃ during the oxy-fuel combustion of methane in a plug flow reactor (T=973-1773 K, P=1 atm)

and used a detailed chemical kinetic model to interpret their results [11]. Reaction products like NO, CO and CO₂ were quantified through a series of continuous gas analyzers. This study showed that a high CO₂ level (90%) enhanced NO formation under reducing conditions, while it inhibited NO production under stoichiometric and lean conditions. According to the authors, the enhanced CO concentrations and alteration in the amount and partitioning of O/H radicals were responsible for the effect of the high CO₂ concentration on the NH₃ conversion. More recently, Barbas et al. [12] focused on the oxy-fuel combustion of methane doped with ammonia at temperatures ranging from 1200-1900 K in a premixed laminar flame with detection of O₂, CO, CO₂, total hydrocarbons and NO_x. They observed a decrease of the mole fractions of CO and NO under fuel-lean conditions. According to this study, NO is mainly formed from the reaction of HNO with H under these conditions.

Despite the abundant experimental data on ammonia addition during methane combustion, to our knowledge, there is no systematic experimental study of the influence of operating variables such as ammonia concentration and temperature. The present study focuses on the oxidation of methane doped with ammonia from low to high temperatures in a jet-stirred reactor. Although the doping effect of several species on methane combustion has been previously studied, the role of ammonia in such kind of configuration is quite novel, and has never been studied so far.

Experimental method

Experiments were carried out in a fused silica jet-stirred reactor (JSR), a type of continuous stirred-tank reactor operated at steady state (constant temperature, pressure, residence time and inlet flow composition). This type of reactor was used for numerous gas phase kinetic studies and the present JSR setup was already described in previous papers [13,14]. Briefly, the jet-stirred reactor consists in a spherical vessel with injection of the fresh mixture through four nozzles

* Corresponding author: olivier.herbinet@univ-lorraine.fr
Proceedings of the European Combustion Meeting 2019

located at the center of the reactor. It was designed to obtain four turbulent jets, which provide a good mixing of the gas phase and an homogeneous composition. The fresh mixture is preheated to ensure the temperature homogeneity of the gas phase. As a result, the JSR can be modeled as a perfectly stirred reactor. Bronkhorst mass flow controllers are used for reactor feeding (relative uncertainty of $\pm 0.5\%$ in flow rates, affecting the residence time: 1.5 ± 0.1 s). The heating of the reactor is achieved through Inconel Thermocoax resistances and the reaction temperature is measured with a K-type thermocouple located in a glass finger close to the center of the reactor (uncertainty of ± 5 K). A scheme of the experimental facility is shown in Figure 1.

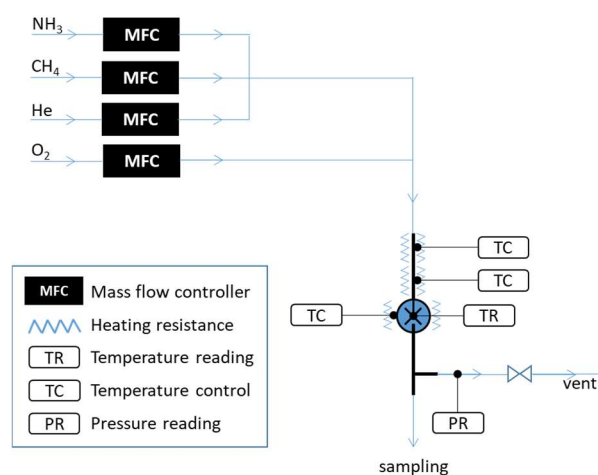


Fig. 1. Scheme of the experimental facility.

Several diagnostics were used for the analysis of the reactants and reaction products. A gas chromatograph equipped with a GSQ capillary column and a flame ionization detector preceded by a methanizer (for the reduction by H_2 of oxygenated functional groups over a heated nickel catalyst) was used for the quantification of carbon containing species like methane, carbon monoxide, carbon dioxide and the three C_2 hydrocarbons (the carrier gas was helium). In the present study, the methanizer allowed a better sensitivity for carbon monoxide and carbon dioxide detection than a thermal conductivity detector as these species are transformed into methane over the catalyst. Nitric oxide (NO) and nitrogen dioxide (NO_2) were detected using a dedicated NO_x analyzer (Thermo Scientific Model 42i). The detection is based on chemiluminescence (reaction of nitric oxide with ozone releasing photons). This analyzer has two channels, one for the detection of nitric oxide in a direct and independent way, and a second one for the measure of the total NO_x concentration. In the second channel, the sampled gas passes over a heated catalyst transforming nitrogen oxides to nitric oxide, which is detected by chemiluminescence as in the first channel. The nitrogen dioxide concentration is then indirectly obtained by subtraction. For ammonia, the quantification was performed using an advanced spectroscopic technique: continuous-wave cavity ring-down spectroscopy. This technique was successfully

used for the detection of species like hydrogen peroxide during the oxidation of alkanes [15] and HONO during the oxidation of *n*-pentane doped with nitric oxide [16]. Ammonia has strong absorption lines in the wavelength range $6637\text{--}6643\text{ cm}^{-1}$ making the quantification accurate and providing a good sensibility. Relative uncertainties in mole fractions are $\pm 5\%$ for species detected by gas chromatography and nitric oxide. It is $\pm 10\%$ for ammonia and nitrogen dioxide.

Kinetic modeling

The kinetic mechanism used to interpret the experimental results was set up starting from the CRECK framework [17], describing the pyrolysis, partial oxidation and combustion of hydrocarbon fuels up to C_{16} . Methane mechanism was initially developed by Ranzi et al. [18]. Here, the use of an approach based on reaction classes allowed the systematical evaluation of the reaction rates of H-abstractions and isomerizations. The core mechanism was recently updated by including the H_2/O_2 and C_1/C_2 mechanisms developed by Metcalfe et al. [19], and C_3 subset of Burke et al. [20]. Thermodynamic properties were updated by using the database by Burcat and Ruscic [21].

Concerning ammonia submechanism, it was conceived starting from the NO_x subset, which was recently updated, too [14]. Initiation reactions with and without oxygen were taken from the review works of Baulch [22] and Dean and Bozzelli [23], respectively. Pyrolysis mechanism was taken from the works of Davidson et al. [24] and Klippenstein et al. [25], respectively. Reaction rates and branching ratio of NO reduction via NH_3 were taken from Klippenstein [26]. Finally, the direct interaction of ammonia with methane, i.e. methane initiation via H-abstraction by ammine radical ($NH_2 + CH_4 = CH_3 + NH_3$) was included, following the calculations of Song et al. [27].

The overall mechanism includes 160 species and 2476 reactions. Both methane and ammonia mechanism were separately validated. As for ammonia, its validations are summarized in Figure 2. In both cases, a satisfactory agreement is observed with experimental data under a wide range of operating conditions: ignition delay times were correctly reproduced under lean-to-rich conditions, as well as for pressures up to 30 atm. Similarly, laminar flame speeds were accurately predicted over the whole range of equivalence ratios.

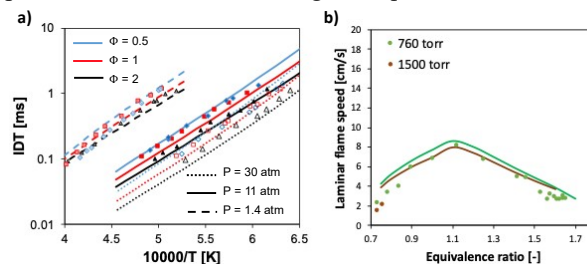


Fig. 2. Validation of NH_3 mechanism. a) Ignition delay time of NH_3/O_2 mixtures, diluted with 99% Ar. b) Laminar flame speed ($T_{in} = 298$ K). Experimental data from [28,29].

Experimental results

Experiments were carried out over the temperature range 500-1200 K, at a residence time of 1.5 s, a pressure of 106.7 kPa (800 Torr), with inlet methane and ammonia mole fractions of 10000 and 500 ppm, respectively, and at three equivalence ratios (0.5, 1 and 2).

Two particular phenomena were observed during experiments, making the oxidation study of methane/ammonia mixtures tricky. The first phenomenon was the occurrence of oscillation regimes under some conditions (at the highest temperatures for the lean and stoichiometric mixtures). The steady state could not be reached, and mole fractions were not constant in time, which was not compatible with the diagnostics used in this study. This explains why the temperature range is limited for some conditions in the results displayed hereafter. This phenomenon has already been reported in literature before for the oxidation of neat methane [30]. The second phenomenon was the occurrence of wall reactions strongly enhancing the ammonia consumption, although the reactor was made of fused silica. This problem was overcome by treating the surface of the JSR before each experiment by flowing all gases but ammonia under reactive conditions.

Obtained mole fraction temperature dependence is displayed in Figures 3-6. The temperature for the reactivity onset is very sensitive to the equivalence ratio: it is about 1000 K for the lean condition, 1075 K for the stoichiometric one, and 1150 K for the rich one, according to mole fractions of methane and ammonia shown in Figure 3. Figure 3 also displays the fuel mole fraction in the case of the oxidation of neat methane. Mole fractions are similar to those of methane when doped with ammonia for the stoichiometric and rich conditions, whereas the reactivity is clearly enhanced under lean conditions.

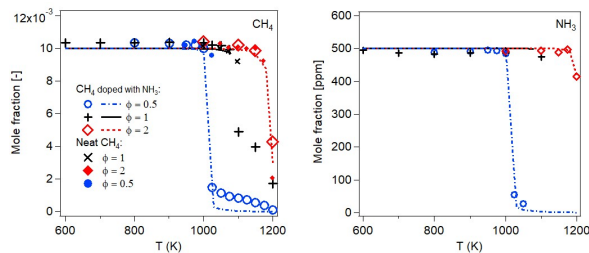


Fig. 3. Temperature dependence of the mole fractions of methane and ammonia as a function of the temperature at the three studied equivalence ratios (0.5, 1 and 2) for the oxidation of methane doped with ammonia.

The main carbon containing products are carbon monoxide, carbon dioxide, ethylene and ethane (Figure 4). Under lean conditions, carbon monoxide peaks at 1025 K. Above this temperature, a decrease of the carbon monoxide mole fraction is observed, with a simultaneous increase of the mole fraction of carbon dioxide. Mole fractions of ethylene and ethane remain low (less than 500 ppm). A larger equivalence ratio favors the formation of unburnt species.

Only two nitrogen containing species were detected during this study: nitric oxide (NO) and nitrogen dioxide

(NO₂), but one or several additional N-containing species are likely formed because the N-atom balance is not closed. Mole fractions of nitric oxide and nitrogen dioxide are displayed in Figure 5. Under lean conditions, mole fractions of nitric oxide and nitrogen dioxide increase simultaneously to the ammonia depletion. Nitrogen dioxide already peaks at 1025 K. Then nitrogen dioxide mole fractions decrease whereas those of nitric oxide still increase. Note that nitrogen dioxide behaves closely to carbon monoxide whereas nitric oxide behaves closely to carbon dioxide.

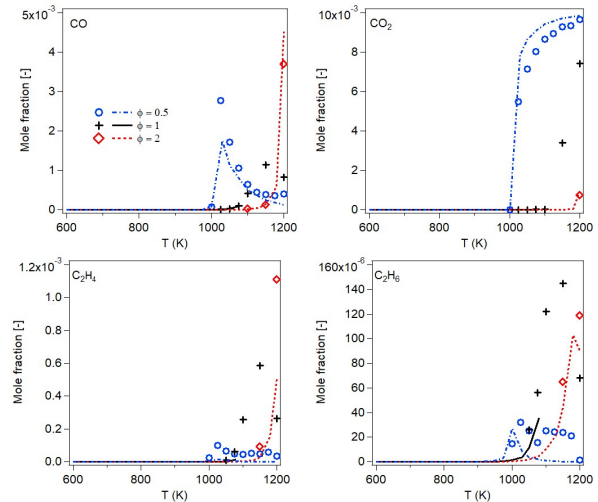


Fig. 4. Temperature dependence of the mole fractions of carbon monoxide, carbon dioxide, ethylene and ethane as a function of the temperature at three equivalence ratios (0.5, 1 and 2) for the oxidation of methane doped with ammonia.

For the stoichiometric condition, oscillation behavior was detected for some conditions and data displayed above 1025 K are not accurate. Indeed oscillations are not compatible with the spectrum acquisition time of ammonia (about 30 min). The acquisition of data for nitric oxide and nitrogen dioxide is much faster (a few tens of seconds), but still not enough to obtain reliable values. The values displayed in Figure 5 for nitric oxide and nitrogen dioxide are sort of an average, whose evolution range is not known (the amplitude of oscillations depends on the conditions). Oscillations seem to have less impact on species like methane, carbon monoxide and carbon dioxide. This is because mole fractions of these species are larger compared to those of nitric oxide and nitrogen dioxide.

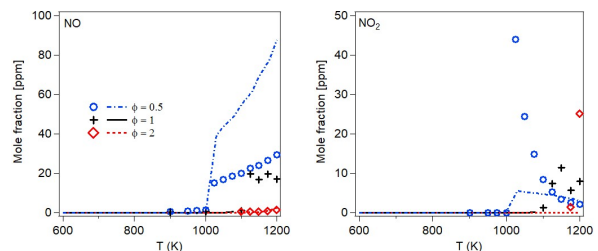


Fig. 5. Temperature dependence of the mole fractions of nitric oxide and nitrogen dioxide as a function of the temperature at the three studied equivalence ratios (0.5, 1 and 2) for the oxidation of methane doped with ammonia.

Experiments were also performed for neat ammonia (fuel inlet mole fraction of 500 ppm) in the presence of oxygen (20 000 and 40 000 ppm) and under reductive atmosphere (pyrolysis). Data are displayed in Figure 6. For the oxidation, reactivity is observed from 1050 to 1075 K. The reactivity of neat ammonia is clearly lower than in the presence of methane (whereas the amount of oxygen was kept constant for comparison). For the pyrolysis, no reactivity was observed over the investigated temperature range. For oxidation, the only products which was detected was nitric oxide (no NO₂ was detected, whatever the temperature and the equivalence ratio). NO mole fractions were relatively low. Other N-atom containing products (e.g., N₂) were likely formed given that NO mole fractions did not allow to close the N-atom balance.

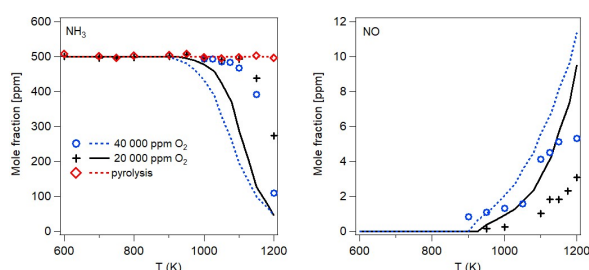


Fig. 6. Temperature dependence of the mole fractions of nitric oxide and nitrogen dioxide as a function of the temperature for the oxidation and pyrolysis of neat ammonia.

Discussion

Experimental data and data computed using the detailed kinetic model described in the kinetic modeling section of this paper are compared in Figures 3-6. Note that the model predicts some oscillation behavior under some conditions. In this case, no steady state solution could be reached and simulation data are not presented in the graphs (this is especially the case for the stoichiometric condition above 1075 K). The detailed kinetic model predicts well the temperature for the reactivity onset as it can be seen for methane and for ammonia in Figure 3, whatever the equivalence ratio. The two fuel conversion temperature dependences are well predicted by the model, except that the conversion of methane is over-estimated for the lean condition at temperatures above 1025 K. Indeed, the model predicts an abrupt consumption of methane with a quasi-total conversion above 1025 K, whereas experimental mole fractions decrease abruptly but not to zero and then keep decreasing but in a smoother way. For neat methane oxidation, the model over-predicts the reactivity of the system with a shift of about 100 K towards lower temperatures (Figure 6). For the pyrolysis, the model predicts no reactivity as it was observed during experiments (Figure 6).

As far as reaction products are concerned, mole fractions of carbon monoxide and of carbon dioxide are well reproduced by the model at all equivalence ratios (Figure 4). Mole fractions of ethylene and ethane are also fairly well reproduced by the model. Discrepancies are observed for nitric oxide and nitrogen dioxide (Figure 5).

For the lean case, the model predicts larger mole fractions for nitric oxide and lower ones for nitrogen dioxide, but the trends are in an overall good agreement. For the rich case, the model predicts no NO₂ whereas it was detected during experiments. Nevertheless the signal detected for NO₂ under these high temperature conditions is suspect and is likely due to an interference of HCN, which is a typical high temperature oxidation products under rich conditions (whereas NO₂ is usually a low-temperature oxidation products).

For the neat ammonia oxidation, the model predicts NO mole fractions in a relative good agreement with experimental data (Figure 6). The model predicts the formation of significant mole fractions of nitrogen (a little bit more than 200 ppm of N₂ at 1200 K with 40 000 ppm of oxygen).

A kinetic analysis of the model was performed to highlight the chemistry involved during the oxidation of methane doped with ammonia and in the oxidation of neat ammonia.

A rate of production analysis for the consumption of methane and ammonia in the case of the oxidation of methane doped with ammonia (at 1025 K, for the lean case, corresponding to conversions of 97.1 and 96.7% of methane and ammonia, respectively) was performed. The analysis shows that the consumption of methane starts with the classic H-atom abstraction reaction $\text{CH}_4 + \text{OH} = \text{CH}_3 + \text{H}_2\text{O}$. The main consumption route of CH₃ is the reaction of CH₃ with NO₂ forming CH₃O + NO, the recombination reaction forming ethane, the reaction with O-atom forming H + CH₂O, and the reaction of CH₃ with HO₂ forming CH₃O + OH. Then the reactions of CH₃O, CH₂O, CHO, CO leading to CO₂ are not affected by the presence of ammonia. Figure 7 displays a reaction scheme for the consumption path of ammonia. Ammonia is mainly consumed by H-atom abstraction with OH radicals to form NH₂ radicals and water. Two channels mainly consume NH₂ radicals: first, a reaction with HO₂ radicals leading to H₂NO + OH; second, a reaction with NO giving N₂ and water. Note that N₂ could not be detected during experiments, because its mole fractions were below the detection limit of the gas chromatograph used for the detection of this species. Less important routes for the consumption of NH₂ (not shown in Figure 7) are the H-atom abstraction from methane, the recombination with CH₃, the reaction with NO to OH + NNH (giving N₂ + H), and the reaction with O-atom yielding H + HNO (reactions of HNO are described hereafter). Back to H₂NO, it reacts with OH by H-atom abstraction to form HNO and water. Then HNO leads to NO through two different H-atom abstraction reaction: first with O₂, second with methyl radicals.

Under the same conditions as those used for the rate of production analysis of Figure 7, the model predicts a conversion of only 22.4% for neat ammonia. This prove that the reaction of methane enhances the reactivity of ammonia. The consumption path diagram is very similar to that displayed in Figure 7, except that HNO only reacts with O₂ to form NO. The H-atom abstraction with methane and the recombination with CH₃ are no longer

possible for the NH_2 radical. At 1200K (conversion of 91.0% for ammonia), the consumption path scheme is also very similar, except that H_2NO also reacts with O_2 forming HNO and HO_2 .

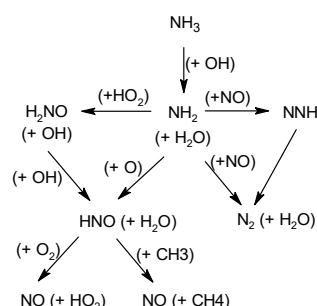


Fig. 7. Rate of production analysis for the consumption of ammonia in the case of the oxidation of methane doped with ammonia (1025 K, equivalence ratio of 0.5).

A sensitivity analysis was performed for ammonia in the presence of methane under the conditions of Figure 7. It is displayed in Figure 8. Except the usual branching reaction $\text{H}+\text{O}_2=\text{O}+\text{OH}$, the second reaction having a positive effect on the consumption of ammonia is the H-atom abstraction of ammonia by OH producing NH_2 and water. Other reactions with a positive effect on the consumption of ammonia are in a general way reactions converting small species in more reactive ones, such as CH_3+NO_2 giving $\text{CH}_3\text{O}+\text{NO}$ and HO_2+NO leading to $\text{OH}+\text{NO}_2$. The reactions which have a negative effect on the consumption of methane are usual reactions converting reactive species into less reactive ones like $\text{H}+\text{O}_2(+\text{M})$ to $\text{HO}_2(+\text{M})$ and $\text{OH}+\text{NO}$ to $\text{H}+\text{NO}_2$.

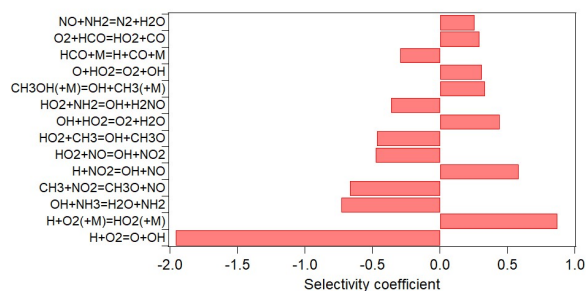


Fig. 8. Sensitivity analysis for NH_3 in the case of the oxidation of methane doped with ammonia (1025 K, equivalence ratio of 0.5).

Figure 9 displays the sensitivity analysis for methane, also under the conditions of Figure 7. The selectivity diagram is very similar to that of ammonia in Figure 8. This shows that the reactivity of both species is driven by the global reactivity of the system and that there is very little direct interactions between ammonia and methane specific oxidation chemistries, but that NO plays an important role in the global reactivity of the system.

The sensitivity analysis for NO is shown in Figure 10. The two reactions having the most positive effect on the mole fraction of NO are the reaction of NH_2 with HO_2 forming H_2NO and OH, and the usual branching reaction $\text{H}+\text{O}_2=\text{O}+\text{OH}$ enhancing the global reactivity. The reaction $\text{NH}_2+\text{HO}_2=\text{H}_2\text{NO}+\text{OH}$ competes with reactions

inhibiting the formation of NO like the two reactions of NH_2 with NO leading to N_2 and water, and to $\text{NNH}+\text{OH}$.

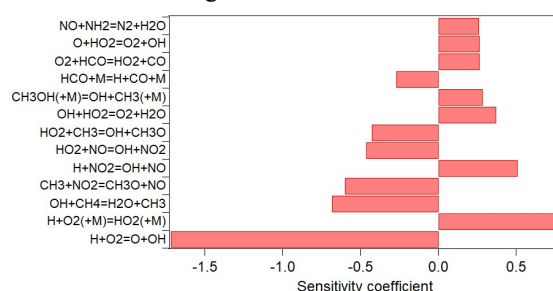


Fig. 9. Sensitivity analysis for CH_4 in the case of the oxidation of methane doped with ammonia (1025 K, equivalence ratio of 0.5).

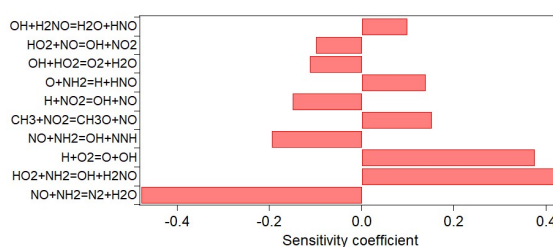


Fig. 10. Sensitivity analysis for NO in the case of the oxidation of methane doped with ammonia (1025 K, equivalence ratio of 0.5).

Conclusions

The oxidation of methane doped with ammonia was experimentally and theoretically studied to better understand the interactions between these two molecules in combustion processes fed with biogas. Experiments were carried out in a jet-stirred reactor operated at steady state, at a residence time of 1.5 s, a pressure of 800 Torr and over the temperature range 500-1200 K. The inlet flow composition was 10 000 ppm of methane and 500 ppm of ammonia. Three equivalence ratios were investigated: 0.5, 1 and 2, with dilution into helium. Several diagnostics were used to quantify reaction products. Gas chromatography was used for the quantification of carbon containing species like methane, CO, CO_2 and the C_2 hydrocarbons. A NO_x analyzer was used for the detection of NO and NO_2 . Ammonia quantification was performed using an advanced spectroscopic technique: continuous-wave cavity ring-down spectroscopy. The occurrence of wall effects enhancing the ammonia consumption was observed under some conditions, although the reactor was made of fused silica. This problem was overcome by treating the surface before each experiments. The comparison of these data with data obtained for neat methane under the similar conditions did not show any significant influence of ammonia on the reactivity of methane except under lean conditions where the reactivity was enhanced. All these data were satisfactorily compared with data computed using a model developed by Politecnico di Milano. The model catches well the reactivity of methane and ammonia, as well as the effect of the equivalence ratio on the reactivity temperature window. Finally, the kinetic analysis of the system shed light on the underlying causes of the anticipated ignition, and the

major role of NO in anticipating methane reactivity. Although the effect of NO as a doping species had been already established in previous works [14], it was observed that even as an intermediate species in the ammonia oxidation path, it affects methane oxidation to a major extent, shifting the reactor ignition by up to ~100 K, especially in leaner conditions.

Acknowledgements

This work has received funding from the European Union H2020 (H2020-SPIRE-04-2016) under grant agreement n°723706.

References

- [1] D.P.B.T.B. Strik, A.M. Domnanovich, P. Holubar, A pH-based control of ammonia in biogas during anaerobic digestion of artificial pig manure and maize silage, *Process Biochem.* 41 (2006) 1235–1238. doi:10.1016/j.procbio.2005.12.008.
- [2] R.O. Arazo, D.A.D. Genuino, M.D.G. de Luna, S.C. Capareda, Bio-oil production from dry sewage sludge by fast pyrolysis in an electrically-heated fluidized bed reactor, *Sustain. Environ. Res.* 27 (2017) 7–14. doi:10.1016/j.serj.2016.11.010.
- [3] P. Glarborg, A.D. Jensen, J.E. Johnsson, Fuel nitrogen conversion in solid fuel fired systems, *Prog. Energy Combust. Sci.* 29 (2003) 89–113. doi:10.1016/S0360-1285(02)00031-X.
- [4] T. Hasegawa, M. Sato, Study of Ammonia Removal from Coal-Gasified Fuel, *Combust. Flame.* 114 (1998) 246–258. doi:10.1016/S0010-2180(97)00315-5.
- [5] A.A. Konnov, I.V. Dyakov, J.D. Ruyck, Probe Sampling Measurements of No in CH₄+O₂+N₂ Flames Doped with NH₃, *Combust. Sci. Technol.* 178 (2006) 1143–1164. doi:10.1080/00102200500296788.
- [6] B. Li, Y. He, Z. Li, A.A. Konnov, Measurements of NO concentration in NH₃-doped CH₄+air flames using saturated laser-induced fluorescence and probe sampling, *Combust. Flame.* 160 (2013) 40–46. doi:10.1016/j.combustflame.2012.10.003.
- [7] B.A. Williams, J.W. Fleming, Radical species profiles in low-pressure methane flames containing fuel nitrogen compounds, *Combust. Flame.* 110 (1997) 1–13. doi:10.1016/S0010-2180(97)00063-1.
- [8] I. Rahinov, A. Goldman, S. Cheskis, Absorption spectroscopy diagnostics of amidogen in ammonia-doped methane/air flames, *Combust. Flame.* 145 (2006) 105–116. doi:10.1016/j.combustflame.2005.11.004.
- [9] A. Garo, C. Hilaire, D. Puechberty, Experimental Study of Methane-Oxygen Flames Doped with Nitrogen Oxide or Ammonia. Comparison with Modeling, *Combust. Sci. Technol.* 86 (1992) 87–103. doi:10.1080/00102209208947189.
- [10] P.F. Henshaw, T. D'Andrea, K.R.C. Mann, D.S.-K. Ting, Premixed Ammonia-Methane-Air Combustion, *Combust. Sci. Technol.* 177 (2005) 2151–2170. doi:10.1080/00102200500240695.
- [11] T. Mendiara, P. Glarborg, Ammonia chemistry in oxy-fuel combustion of methane, *Combust. Flame.* 156 (2009) 1937–1949. doi:10.1016/j.combustflame.2009.07.006.
- [12] M. Barbas, M. Costa, S. Vranckx, R. Fernandes, Experimental and kinetic modeling study of CO and NO formation under oxy-fuel conditions, in: 2015: pp. 16–20.
- [13] F.H. Vermeire, H.-H. Carstensen, O. Herbinet, F. Battin-Leclerc, G.B. Marin, K.M. Van Geem, Experimental and modeling study of the pyrolysis and combustion of dimethoxymethane, *Combust. Flame.* 190 (2018) 270–283. doi:10.1016/j.combustflame.2017.12.001.
- [14] Y. Song, L. Marrodán, N. Vin, O. Herbinet, E. Assaf, C. Fittschen, A. Stagni, T. Faravelli, M.U. Alzueta, F. Battin-Leclerc, The sensitizing effects of NO₂ and NO on methane low temperature oxidation in a jet stirred reactor, *Proc. Combust. Inst.* (2018). doi:10.1016/j.proci.2018.06.115.
- [15] C. Bahrini, O. Herbinet, P.-A. Glaude, C. Schoemaecker, C. Fittschen, F. Battin-Leclerc, Quantification of Hydrogen Peroxide during the Low-Temperature Oxidation of Alkanes, *J. Am. Chem. Soc.* 134 (2012) 11944–11947. doi:10.1021/ja305200h.
- [16] L. Marrodán, Y. Song, O. Herbinet, M.U. Alzueta, C. Fittschen, Y. Ju, F. Battin-Leclerc, First detection of a key intermediate in the oxidation of fuel + NO systems: HONO, *Chem. Phys. Lett.* 719 (2019) 22–26. doi:10.1016/j.cpl.2019.01.038.
- [17] E. Ranzi, A. Frassoldati, R. Grana, A. Cuoci, T. Faravelli, A.P. Kelley, C.K. Law, Hierarchical and comparative kinetic modeling of laminar flame speeds of hydrocarbon and oxygenated fuels, *Prog. Energy Combust. Sci.* 38 (2012) 468–501. doi:10.1016/j.pecs.2012.03.004.
- [18] E. Ranzi, A. Sogaro, P. Gaffuri, G. Pennati, T. Faravelli, A Wide-Range Modeling Study of Methane Oxidation, *Combust. Sci. Technol.* 96 (1994) 279–325. doi:10.1080/00102209408935359.
- [19] W.K. Metcalfe, S.M. Burke, S.S. Ahmed, H.J. Curran, A Hierarchical and Comparative Kinetic Modeling Study of C1 – C2 Hydrocarbon and Oxygenated Fuels, *Int. J. Chem. Kinet.* 45 (2013) 638–675. doi:10.1002/kin.20802.
- [20] S.M. Burke, U. Burke, R. Mc Donagh, O. Mathieu, I. Osorio, C. Keesee, A. Morones, E.L. Petersen, W. Wang, T.A. DeVerter, M.A. Oehlschlaeger, B. Rhoads, R.K. Hanson, D.F. Davidson, B.W. Weber, C.-J. Sung, J. Santner, Y. Ju, F.M. Haas, F.L. Dryer, E.N. Volkov, E.J.K. Nilsson, A.A. Konnov, M. Alrefae, F. Khaled, A. Farooq, P. Dirrenberger, P.-A. Glaude, F. Battin-Leclerc, H.J. Curran, An experimental and modeling study of propene oxidation. Part 2: Ignition delay time and flame speed measurements, *Combust. Flame.* 162 (2015) 296–314. doi:10.1016/j.combustflame.2014.07.032.
- [21] A. Burcat, B. Ruscic, Chemistry, T.-I.I. of Tech, Third millenium ideal gas and condensed phase thermochemical database for combustion (with update from active thermochemical tables), Argonne National Lab. (ANL), Argonne, IL (United States), 2005. doi:10.2172/925269.
- [22] D.L. Baulch, C.T. Bowman, C.J. Cobos, R.A. Cox, T. Just, J.A. Kerr, M.J. Pilling, D. Stocker, J. Troe, W. Tsang, R.W. Walker, J. Warnatz, Evaluated Kinetic Data for Combustion Modeling: Supplement II, *J. Phys. Chem. Ref. Data.* 34 (2005) 757–1397. doi:10.1063/1.1748524.
- [23] A.M. Dean, J.W. Bozzelli, Combustion Chemistry of Nitrogen, in: W.C. Gardiner (Ed.), *Gas-Phase Combust. Chem.*, Springer New York, New York, NY, 2000: pp. 125–341. doi:10.1007/978-1-4612-1310-9_2.
- [24] D. Davidson, K. Kohsehoinghaus, A. Chang, R. Hanson, A Pyrolysis Mechanism for Ammonia, *Int. J. Chem. Kinet.* 22 (1990) 513–535. doi:10.1002/kin.550220508.
- [25] S.J. Klippenstein, L.B. Harding, B. Ruscic, R. Sivaramakrishnan, N.K. Srinivasan, M.-C. Su, J.V. Michael, Thermal Decomposition of NH₂OH and Subsequent Reactions: Ab Initio Transition State Theory and Reflected Shock Tube Experiments, *J. Phys. Chem. A.* 113 (2009) 10241–10259. doi:10.1021/jp905454k.
- [26] S.J. Klippenstein, From theoretical reaction dynamics to chemical modeling of combustion, *Proc. Combust. Inst.* 36 (2017) 77–111. doi:10.1016/j.proci.2016.07.100.
- [27] S.H. Song, D.M. Golden, R.K. Hanson, C.T. Bowman, J.P. Senosiain, C.B. Musgrave, G. Friedrichs, A shock tube study of the reaction NH₂+CH₄ → NH₃+CH₃ and comparison with transition state theory, *Int. J. Chem. Kinet.* 35 (2003) 304–309. doi:10.1002/kin.10131.
- [28] O. Mathieu, E.L. Petersen, Experimental and modeling study on the high-temperature oxidation of Ammonia and related NO_x chemistry, *Combust. Flame.* 162 (2015) 554–570. doi:10.1016/j.combustflame.2014.08.022.
- [29] P. Ronney, Effect of Chemistry and Transport-Properties on Near-Limit Flames at Microgravity, *Combust. Sci. Technol.* 59 (1988) 123–141. doi:10.1080/00102208808947092.
- [30] M. Lubrano Lavadera, Y. Song, P. Sabia, O. Herbinet, M. Pelucchi, A. Stagni, T. Faravelli, F. Battin-Leclerc, M. de Joannon, Oscillatory Behavior in Methane Combustion: Influence of the Operating Parameters, *Energy Fuels.* 32 (2018) 10088–10099. doi:10.1021/acs.energyfuels.8b00967.